Available online at www.sciencedirect.com
SCIENCE DIRECT®
PERGAMON
Solid-State Electronics 47 (2003) 205–212
SOLID-STATE ELECTRONICS
www.elsevier.com/locate/sse

Temperature-insensitive semiconductor quantum dot laser

Levon V. Asryan [a,b,*], Serge Luryi [a]

[a] Department of Electrical and Computer Engineering, State University of New York at Stony Brook, Stony Brook, NY 1794-2350, USA
[b] Ioffe Physico-Technical Institute, St. Petersburg 194021, Russia

Received 19 January 2002; received in revised form 28 March 2002; accepted 27 April 2002

Abstract

Different approaches to the design of a genuinely temperature-insensitive quantum dot (QD) laser are proposed. Suppression of the parasitic recombination outside the QDs, which is the dominant source of the temperature dependence of the threshold current in the conventional design of a QD laser, is accomplished either by tunneling injection of carriers into the QDs or by band-gap engineering. Elimination of this recombination channel alone enhances the characteristic temperatures T_0 above 1000 K. Remaining sources of temperature dependence (recombination from higher QD levels, inhomogeneous line broadening, and violation of charge neutrality in QDs) are studied. Tunneling-injection structures are shown to offer an additional advantage of suppressed effects of inhomogeneous broadening and neutrality violation.

Keywords: Quantum dot lasers; Semiconductor heterojunctions; Tunneling

1. Introduction

High temperature stability of operation is an essential feature required of long wavelength semiconductor heterostructure lasers for telecommunications. Commercial lasers with either bulk or quantum well (QW) active regions suffer from rather poor temperature stability. The all-important parameter T_0, which describes empirically the T-dependence of the threshold current density j_{th} and is defined as $T_0 = 1/(\partial \ln j_{th}/\partial T)$, does not exceed 100 K in best commercial lasers. Quantum dot (QD) lasers, exploiting zero-dimensional (0D) active medium were proposed years ago [1,2] and one of their main predicted advantages was high temperature stability. Nevertheless, despite significant recent progress in the fabrication of QD lasers [3–12], their temperature stability has fallen far short of expectations. Although the best results for T_0 in QD lasers are quite respectable, matching and even exceeding the best QW results at room temperature, so far they have been nowhere near the predicted "infinite" values that would allow regarding the laser as temperature insensitive.

In all semiconductor diode lasers, electrons and holes are injected from 3D contact regions, where carriers are free, into an active region, where lasing transitions take place and where carriers may be dimensionally confined. At relatively high temperatures (300 K and above), the dominant source of the T-dependence of j_{th} in all semiconductor lasers originates from carriers that do not contribute to the lasing transition. In lasers with 3D (bulk) or 2D (QW) active regions, there is always a population of carriers distributed according to Fermi–Dirac statistics within some energy range (determined by the temperature and the injection level) around the lasing transition energy (Fig. 1). These carriers reside in the active region itself and their recombination contributes to a T-dependent threshold.

* Corresponding author. Address: Department of Electrical and Computer Engineering, State University of New York at Stony Brook, Stony Brook, NY 11794-2350, USA. Tel.: +1-631-632-84-22; fax: +1-631-632-84-94.
E-mail addresses: asryan@ece.sunysb.edu (L.V. Asryan), s.luryi@ece.sunysb.edu (S. Luryi).

0038-1101/02/$ - see front matter
PII: S0038-1101(02)00196-X

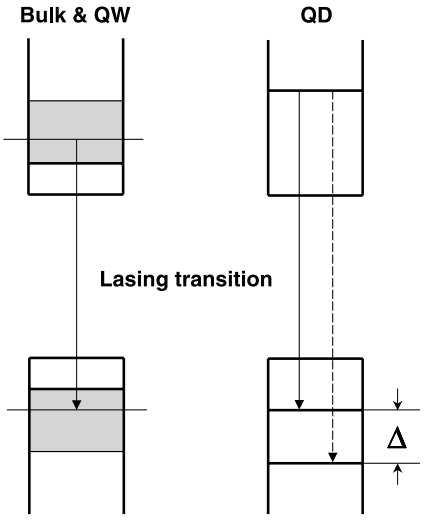

Fig. 1. Carrier population in bulk, QW, and single QD. The dashed arrow shows the excited-state transition in a QD.

It is the absence of parasitic recombination in the active medium itself that gave rise to the original hopes of ultra-high temperature stability in QD lasers, where optical transitions occur between discrete levels. However, in all conventional QD laser designs the problem of parasitic recombination has not been removed.

This recombination arises primarily from carriers residing in layers adjacent the active medium, primarily in the optical confinement layer (OCL). Consider the conventional QD laser heterostructure (Fig. 2). Carriers are injected from cladding layers into the OCL where an approximate equilibrium with the QDs is established at room temperature. High occupation of QD electron and hole levels embedded in the OCL is therefore accompanied by an appreciable 3D population of both types of carriers in the OCL itself. These carriers give rise to a temperature-dependent recombination current while not contributing to the lasing. Such a mechanism of T-dependence is also present in other semiconductor lasers, but in QD lasers it plays the central role at room temperature.

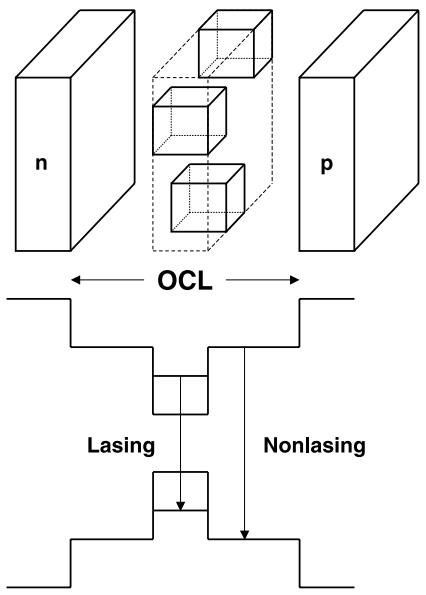

Fig. 2. Schematic view and energy band diagram of a conventional QD laser.

Another source of T-dependence arises from the fact that not all QDs are alike. Owing to the unavoidable inhomogeneous broadening, a sizeable fraction of them does not contribute to the lasing transition while still adding to the parasitic recombination. As far as T_0 is concerned, this effect is similar to that due to carriers residing in the OCL. Despite the impressive recent progress in controlling QD parameters during epitaxial growth, even the best devices show a significant QD size dispersion, as indicated by the measured gain and spontaneous emission spectra. Thus, rather uniform QD ensembles are characterized by the relative QD size fluctuations of $\pm 5\%$ about the mean (to the overall QD size fluctuations of about 2–2.5 monolayers) [13–15]. The effect of QD size dispersion on the threshold current and its T-dependence was first considered in [16] and [17], respectively. If we define separately the characteristic temperatures T_0^{QD} and T_0^{out} for the threshold current components associated with the recombination inside the QDs [$j_{\mathrm{QD}}(T)$] and outside the QDs, we find that T_0^{QD} is much higher than T_0^{out}. Indeed, the value of T_0^{out} is below 100 K at room temperature [17], whereas the calculated value of T_0^{QD} due to inhomogeneous broadening is over 1500 K [18]. We see that the effect of QD size dispersion is relatively small compared to the OCL recombination. The reciprocal of the characteristic temperature can be written as follows:

$$\frac{1}{T_0} = \frac{j_{\mathrm{QD}}}{j_{\mathrm{th}}}\frac{1}{T_0^{\mathrm{QD}}} + \left(1 - \frac{j_{\mathrm{QD}}}{j_{\mathrm{th}}}\right)\frac{1}{T_0^{\mathrm{out}}} \tag{1}$$

where $j_{\mathrm{QD}}/j_{\mathrm{th}}$ is the QD fraction of the threshold current density. The characteristic temperature T_0 increases dramatically with increasing $j_{\mathrm{QD}}/j_{\mathrm{th}}$ as can be seen from the plot in Fig. 3. When the entire injection current is consumed in QDs, the dominant remaining contribution to temperature dependence is from inhomogeneous broadening and the characteristic temperature $T_0 = T_0^{\mathrm{QD}}$ should be very high.

Thus we can expect that suppression of the OCL recombination alone will result in a dramatic improvement of the temperature stability. One way of accomplishing this is based on tunneling injection of carriers into the QDs that was proposed in [18]. This design,

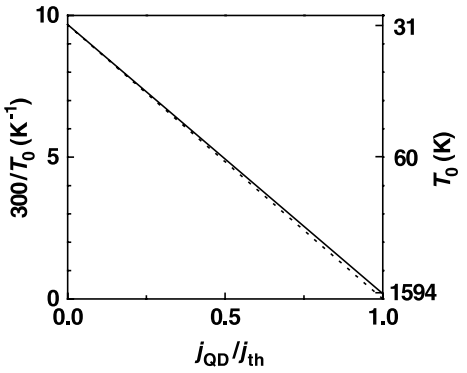

Fig. 3. Characteristic temperature against the QD fraction of the threshold current density at room temperature. The dotted line depicts $1/T_0$ in the absence of inhomogeneous line broadening ($T_0^{QD} = \infty$). The values of T_0 are indicated on the right axis.

shortly discussed in Section 2, allows both suppressing the parasitic components of threshold current and diminishing the effect of inhomogeneous line width. In this paper, we propose an alternative novel approach (Section 3), which suppresses the parasitic recombination by introducing heterojunction barriers that block the passage of minority carriers into the "wrong" side of the QD layer while remaining transparent for majority-carrier injection into the QDs themselves. This approach is based on independent variations of the barrier heights for electrons and holes and allows eliminating parasitic recombination in the OCL without utilizing the concept of tunneling injection. Relative merits of these two approaches are discussed and the remaining sources of temperature dependence (recombination from higher QD levels and violation of charge neutrality (VCN) in QDs) are studied quantitatively (Section 4) in addition to inhomogeneous line broadening considered in [18].

Recent experimental results related to our concept of a tunneling-injection QD laser are discussed in Section 5 and our conclusions are summarized in Section 6.

2. Tunneling-injection temperature-insensitive QD laser

A schematic view of the structure and its energy band diagram are shown in Fig. 4. Basically, we have a separate confinement double-heterostructure laser. Electrons and holes are injected from n- and p-cladding layers, respectively. The QD layer, located in the central part of the OCL, is clad on both sides by QWs separated from the QDs by thin barrier layers. Injection of carriers into QDs occurs by tunneling from the QWs.

The key idea of the device is that the QWs themselves are not connected by a current path that bypasses the

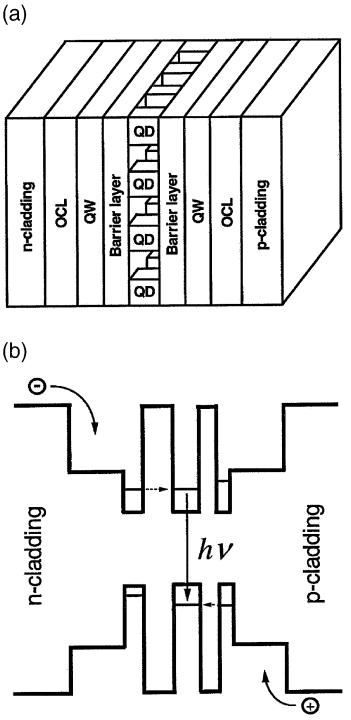

Fig. 4. Schematic view (a) and energy band diagram (b) of a tunneling-injection QD laser. The QWs and the QDs are assumed implemented in the same material, although this does not have to be necessarily the case in general. The electron-injecting QW is wider than the hole-injecting QW and both QWs are narrower than the QD to accomplish resonant alignment of the majority-carrier subbands with the QD energy levels. The tunnel barrier on the electron-injecting side is made thicker to suppress hole leakage from the QD.

QDs. Electrons (coming from the left in Fig. 4) approach the right QW only through the confined states in the QDs. Similarly, holes cannot directly approach the left QW. To realize this idea, the following conditions must be met:

1. The material and the thickness of QWs should be chosen so that the lowest subband edge in the injecting QW matches the quantized energy level for the corresponding type of carrier in the average-sized QD (the QWs may or may not be of the same material as the QDs).
2. The barriers should be reasonably high to suppress thermal emission of carriers from the QWs.
3. The material separating QDs from each other in the QD layer should have sufficiently wide bandgap to suppress all tunneling other than via the QD levels. This material may be the same as that of the barrier layers.
4. The barrier layers should be thin enough to ensure effective tunneling between the QW and QD states. At

the same time, the separation between the adjacent QDs in the QD layer should be large enough to prevent any significant tunnel splitting of the energy levels in neighboring QDs (otherwise, such a splitting would effectively play the same role as the inhomogeneous line broadening).

2.1. Suppression of escape tunneling

We should note that a fraction of injected carriers might not recombine in the QD but escape in a second tunneling step into the "foreign" QW and recombine with the majority carriers there. The ratio of the escape tunneling rate to the QD recombination rate is given by

$$\frac{j_{\mathrm{Leak}}}{j_{\mathrm{QD}}} = \frac{\tau_{\mathrm{QD}}}{\tau_{\mathrm{Leak}}} \tag{2}$$

where τ_{QD} and τ_{Leak} are the spontaneous radiative recombination time in QDs and tunneling-mediated leakage time from QDs. Since neither τ_{QD} nor τ_{Leak} depend on T, there should be only a weak temperature dependence of j_{Leak} faithfully following that of j_{QD} (as discussed below, the only remaining source of T-dependence of j_{QD} is due to the inhomogeneous line broadening and the VCN in QDs). Hence, the escape tunneling does not lead to a considerable temperature dependence of threshold current; nevertheless, in a sensible design this form of leakage should be minimized to lower the value of j_{th}.

A possible way of suppressing the escape tunneling is illustrated in Fig. 4(b). It takes advantage of the lower electron effective mass compared to the hole mass, but uses this advantage differently on the electron- and hole-injecting sides of the structure. On the p-side, when the hole level in the QD is aligned with the hole subband in the hole-injecting QW, the electron subband edge in that QW will be necessarily above the electron level in the QD, thus suppressing the tunneling escape of electrons. On the n-side, this trick does not work, since the resonant alignment of the electron subband in the QW and the electron level in the QD does not prevent tunneling of QD holes into the electron-injecting QW. However, due to the effective mass difference, we can design a wider tunnel barrier on the electron-injecting side, such that it effectively suppresses the tunneling escape of holes while still being relatively transparent for electrons.

Suppression of the leakage on both sides can also be organized in a different way. Depending on the heterostructure composition, the barrier heights for electrons and holes can be varied independently. Using this, one can optimize the structure by increasing the barrier height for out-tunneling particles while keeping it low for in-tunneling particles. An exemplary heterostructure that meets this criterion is illustrated in Fig. 5. A layer composition of a candidate material heterostructure for this type of a tunneling-injection QD laser is presented in Table 1. The structure is lattice-matched (except for the QD part). Conduction and valence band offsets for lattice-matched $Ga_xIn_{1-x}As_yP_{1-y}/InP$ heterojunctions are calculated from the equations $\Delta E_c/\Delta E_g = 0.39$ and $\Delta E_v/\Delta E_g = 0.61$ [19]. For the lattice-matched $Al_{0.48}In_{0.52}As/Ga_{0.47}In_{0.53}As$ heterojunction, $\Delta E_c = 0.52$ eV is taken from [20–22] and then ΔE_v is calculated.

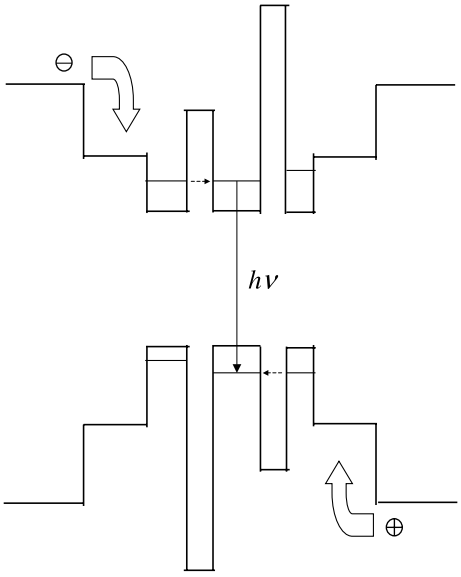

Fig. 5. Energy band diagram of a tunneling-injection QD laser wherein the tunneling leakage is suppressed by independent variation of the barrier heights for electrons and holes.

2.2. Previous tunneling-injection QD laser structures

Carrier injection by tunneling has been previously used in both QW and QD laser designs [23–27]. Tunneling-injection QD laser designs [26,27] were intended primarily to minimize hot carrier effects. Consider the band diagram in Fig. 6, which describes the QD lasers reported in [26,27]. Tunneling-injection barrier on the electron side allows hot electrons to thermalize before entering the QD region. However, a quasi-equilibrium bipolar carrier density and hence substantial parasitic thermo-activated recombination remains on the hole-injecting side of the structure. Therefore, this design does not fully address the issue of temperature sensitivity associated with recombination in the OCL.

3. Temperature-insensitive QD laser by band-gap engineering

Tunneling injection suppresses parasitic recombination by ensuring that the electron density is high where

Table 1
Layer composition of a candidate material heterostructure for a tunneling-injection QD laser of Fig. 5

Layer	Material	E_g (eV)	ΔE_c (eV)	ΔE_v (eV)
n-Cladding	InP	1.35		
			0.133	0.207
OCL	$Ga_{0.2}In_{0.8}As_{0.44}P_{0.56}$	1.01		
			0.114	0.179
QW	$Ga_{0.47}In_{0.53}As$	0.717		
			0.152	0.239
Barrier	$Ga_{0.14}In_{0.86}As_{0.3}P_{0.7}$	1.108		
QDs	InAs	0.36		
			0.52	0.163
Barrier	$Al_{0.48}In_{0.52}As$	1.4		
			0.114	0.179
QW	$Ga_{0.47}In_{0.53}As$	0.717		
			0.133	0.207
OCL	$Ga_{0.2}In_{0.8}As_{0.44}P_{0.56}$	1.01		
p-Cladding	InP	1.35		

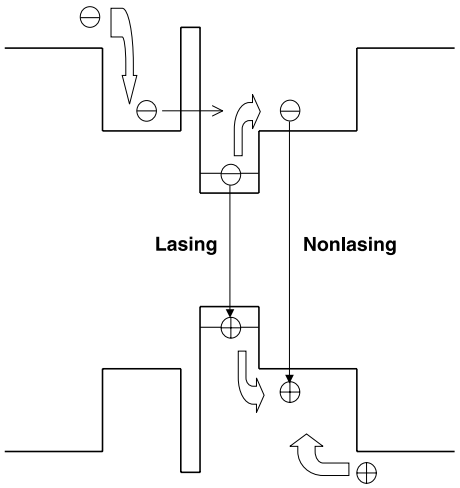

Fig. 6. Schematic band diagram of tunneling-injection QD lasers reported in [26,27]. Carriers of one type only (electrons) are tunneling. The tunneling barrier separates the region where electrons are hot from the rest of the structure containing the active layer with QDs. Electrons thermalize before tunneling through the barrier, so that tunneling electrons—to be captured by QDs—are already cold.

the hole density is negligible and vice versa. However, it is not the only way of accomplishing this goal. An alternative approach can be based on the ability to independently control the potential barriers and fields acting upon electrons and holes in the same physical region.

Consider the structures illustrated in Fig. 7. In these structures the QD layer is embedded in the OCL in such a way that there are only low barriers (Fig. 7(a)) or no barrier at all (Fig. 7(b)) for the injection of electrons (from the left) and holes (from the right) into the QDs. On the other hand, the structures are provided with large "impenetrable" escape barriers that are those blocking electron injection into the right-hand side of the structure, where holes are majority carriers, and hole injection into the left-hand side of the structure where electrons are in abundance. Heterostructure barriers as

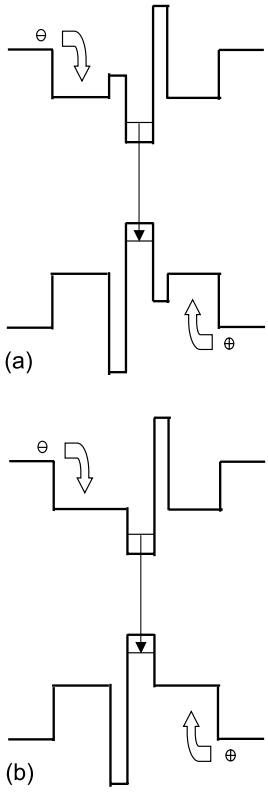

Fig. 7. Prevention of thermo-activated parasitic recombination in the OCL by band-gap engineering. QDs (shown with energy levels) are clad by heterostructure barrier layers that block only the minority-carrier transport.

in Fig. 7(a) can readily be found within the manifold of quaternary III–V heterojunctions, both strained and lattice-matched. The structure in Fig. 7(b) is a "limit case", which serves to illustrate that no barrier for injected carriers is necessary on the injecting side.

The space within the QD layer between the QDs can comprise either of the two barriers or be implemented as a wider gap semiconductor providing blocking of both carrier types.

4. Remaining sources of the temperature sensitivity

In the proposed structures carriers cannot bypass the QDs on their way from one contact to other. This means that QDs play the role of a sole reservoir of electrons (holes) for the OCL regions adjacent to p-cladding (n-cladding). Therefore, the density of minority carriers in these regions will be negligible so that outside the QDs there will be no region in the structure where both electron and hole densities are simultaneously high. The spontaneous radiative recombination rate is hence nonvanishing solely in the QDs. This strongly suppresses the parasitic components of the threshold current, which would otherwise give the main contribution to the temperature dependence.

With the parasitic recombination channels suppressed, we can expect only a slight temperature dependence of j_{th} caused by QD size dispersion, violation of QD neutrality, and by parasitic recombination from higher energy levels in QDs.

4.1. Inhomogeneous line broadening

Calculations [18] show that the characteristic temperature T_0 as limited by the inhomogeneous line broadening is above 1500 K, which is to say the device is practically temperature insensitive for most practical purposes. We emphasize that this dramatic improvement results solely from the suppression of recombination channels outside the active region.

It is interesting to note that the tunneling-injection structures (Figs. 4 and 5) benefit from another still "finer" effect that will further enhance the temperature stability. This effect stems from the resonant nature of tunneling injection and leads to an effective narrowing of the inhomogeneous linewidth. Indeed, tunneling injection inherently selects QDs of the "right" size since it requires the confined-carrier levels to be in resonance with the lowest subband states in the QW. When this condition is met by the QDs of average size, i.e. when QDs with $a = \bar{a}$ are resonant, the number of active QDs is maximized. Consider this situation more closely. For QDs with $a > \bar{a}$ tunneling transitions can only be phonon-mediated. The rates of such transitions are much lower and can be safely neglected. Hence, QDs of sizes larger than the average are effectively cut off. Smaller-size QDs are also cut off, although perhaps less efficiently, because their energy levels would be pumped from higher-momentum states in the injecting QW subband. The higher the in-plane momentum of a 2D-carrier in the QW, the lower is the probability of tunneling transition that results in its capture by the QD.

Selective injection means that those QDs, which do not lase, are not pumped either. As a result, the threshold current will decrease and the temperature stability of j_{th} will be further enhanced.

4.2. Recombination from higher QD levels

If a QD can support excited electron and hole states this can also lead to a thermo-activated parasitic recombination and serve as another source of T-dependence of j_{th}. Denoting the characteristic temperature limited by the presence of excited states in QDs by T_0^{exc}, the ratio T_0^{exc}/T is a universal function of Δ/T (where Δ is the separation of the transition energies in QDs—see Fig. 1). Determination of this function leads to a problem identical to that considered in [18, Appendix] for a bimodal ensemble of QDs. The result is

$$\frac{T_0^{exc}}{T} = \frac{1}{1-r}\,\frac{\left[\left(\frac{1}{f_n}-1\right)\exp\left(\frac{\Delta}{T}\right)+1\right]^3}{2\frac{\Delta}{T}\left(\frac{1}{f_n}-1\right)\exp\left(\frac{\Delta}{T}\right)} \times\left\{rf_n^2+\frac{1-r}{\left[\left(\frac{1}{f_n}-1\right)\exp\left(\frac{\Delta}{T}\right)+1\right]^2}\right\} \tag{3}$$

where f_n is the occupancy of the ground state in QDs, $r = I_1/(I_1+I_2)$, and I_1 and I_2 are the rates of the ground- and excited-state transitions, respectively.

This function is plotted by the solid line in Fig. 8 for a particular value of Δ, chosen so that the minimum of T_0^{exc} would occur at room temperature. From this plot it may appear that recombination from higher QD levels may be the dominant remaining source of T-dependence at room temperature; this is because the excited-state transition rate I_2 was chosen to be equal to that of the ground-state transition and hence $r = 0.5$. However, it should be noted that small enough QDs might not support more than one electronic level even though there may be an excited hole level. Recombination to this level from the ground electron state is suppressed, at least approximately, by the selection rules. Indeed, in a symmetric (cubic) QD this transition is forbidden and while in a realistic (pyramidal) QD this transition is allowed, its rate is suppressed by at least an order of

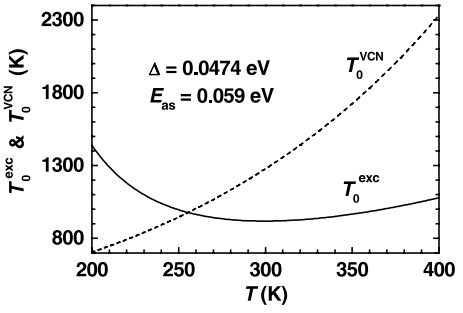

Fig. 8. Characteristic temperature limited by the presence of excited states in QDs (——) and by VCN in QDs (- - -) against temperature.

magnitude ($I_2 < 0.1I_1$) and r is close to unity ($r > 0.9$). We can safely conclude that T-dependence arising from thermally excited higher QD levels is negligible in small enough QD.

4.3. Violation of charge neutrality

The only remaining contribution to temperature dependence of j_{th} results from the VCN in QDs [28]. Unconstrained by neutrality the occupancies of the electron and hole levels in the QD are no longer fixed by the generation condition and become temperature dependent [17]. VCN is the dominant mechanism of temperature sensitivity at low temperatures but it is unimportant at 300 K. Temperature dependence of the characteristic temperature limited by this effect is shown in Fig. 8 by the dashed line. At room temperature the calculated value of T_0 is well over 1000 K.

Note that the dimensionless ratio T_0^{VCN}/T (where T_0^{VCN} is the characteristic temperature limited by VCN in QDs) can also be viewed as a universal function of a dimensionless ratio E_{as}/T. The parameter E_{as} that controls the QD charge depends on the asymmetry of the QD and its environment and is given by $2E_{as} = (F_p + \Delta E_v - \varepsilon_p) - (F_n + \Delta E_c - \varepsilon_n)$, where $\Delta E_{c,v}$ is the band-gap difference between the materials of the cladding layers and QDs, $F_{n,p}$ are the quasi-Fermi levels in n- and p-claddings respectively, and $\varepsilon_{n,p}$ are the quantized energy levels in QDs. Since $F_{n,p}$ depend on T, the parameter of asymmetry E_{as} itself is also T-dependent.

It is again interesting to note that tunneling-injection structures offer an additional advantage. Indeed, the resonant nature of tunneling injection favors a correlation between the occupancies of any given QD by electrons and holes. In an idealized structure, we can expect that all the active QDs will remain neutral and then T_0 will be literally infinite.

5. Recent art

It is encouraging to note recent developments related to our concept of a tunneling-injection QD laser. In [29,30], room-temperature continuous wave (both photopumped and diode) lasing was successfully demonstrated in the InAlP–In(AlGa)P–InP visible-red system ($\lambda = 656$–679 μm), wherein the InP QDs were coupled by resonant tunneling to a single InGaP QW. In the later work [31,32], this idea was realized in the AlGaAs–GaAs–InGaAs–InAs infrared system, wherein the InAs QDs were coupled to the InGaAs QWs. In contrast to [29,30], the QD layer in [31,32] was sandwiched between the two QWs; like the structures in our Figs. 4(b) and 5, the QWs were of different thickness. The use of tunnel coupling of QDs to QW(s) improved the carrier collection and localization in the region of the QDs and reduced the threshold current. In [33], the tunneling transition rate from a QW to a model (disk-shaped) QD was calculated. In [34], introducing the tunnel-injector QW from only the n-side of the structure increased significantly the characteristic temperature of the InGaAs/GaAs QD laser ($T_0 = 237$ K at room temperature).

6. Conclusions

A novel approach to the design of temperature-insensitive lasers proposed earlier [18], has been further developed. The approach, based on blocking the parasitic recombination of carriers outside QDs, offers the possibility of achieving ultra-high temperature stability—which has been the key desired advantage of QD lasers. This can be accomplished in at least two ways by special tailoring of heterostructures that surround the QDs. The simplest way, conceptually, is to introduce potential barriers blocking the minority-carrier transport on both sides of QDs while leaving majority-carrier injection unimpeded. Suppression of the parasitic recombination outside the QDs alone leads to characteristic temperatures T_0 above 1000 K. A particularly favorable way of accomplishing this is by using resonant-tunneling injection of majority carriers. Tunneling injection offers further enhancement of T_0 owing to an inherently suppressed pumping of the nonlasing QDs and correlated occupancies of any given QD by electrons and holes.

Acknowledgements

This work was supported by AFOSR MURI grant F49620-00-1-0331 and Semiconductor Research Corporation (Research ID 612).

References

[1] Dingle R, Henry CH. Quantum effects in heterostructure lasers. U.S. Pat. 3982207, September 21, 1976.
[2] Arakawa Y, Sakaki H. Multidimensional quantum well laser and temperature dependence of its threshold current. Appl Phys Lett 1982;40:939–41.
[3] Kirstädter N, Ledentsov NN, Grundmann M, Bimberg D, Ustinov VM, Ruvimov SS, et al. Low threshold, large T_0 injection laser emission from (InGa)As quantum dots. Electron Lett 1994;30:1416–7.
[4] Mirin R, Gossard A, Bowers J. Room temperature lasing from InGaAs quantum dots. Electron Lett 1996;32:1732–4.
[5] Ledentsov NN, Grundmann M, Heinrichsdorff F, Bimberg D, Ustinov VM, Zhukov AE, et al. Quantum-dot

heterostructure lasers. IEEE J Select Top Quant Electron 2000; 6:439–51.
[6] Bhattacharya P, Klotzkin D, Qasaimeh O, Zhou W, Krishna S, Zhu D. High-speed modulation and switching characteristics of In(Ga)As–Al(Ga)As self-organized quantum-dot lasers. IEEE J Select Top Quant Electron 2000;6: 426–38.
[7] Harris L, Mowbray DJ, Skolnick MS, Hopkinson M, Hill G. Emission spectra and mode structure of InAs/GaAs self-organized quantum dot lasers. Appl Phys Lett 1998; 73:969–71.
[8] Smowton PM, Johnston EJ, Dewar SV, Hulyer PJ, Summers HD, Patane A, et al. Spectral analysis of InGaAs/GaAs quantum-dot lasers. Appl Phys Lett 1999; 75:2169–71.
[9] Huffaker DL, Park G, Zou Z, Shchekin OB, Deppe DG. Continuous-wave low-threshold performance of 1.3-μm InGaAs–GaAs quantum-dot lasers. IEEE J Select Top Quant Electron 2000;6:452–61.
[10] Sugawara M, Mukai K, Nakata Y, Otsubo K, Ishikawa H. Performance and physics of quantum-dot lasers with self-assembled columnar-shaped and 1.3-μm emitting InGaAs quantum dots. IEEE J Select Top Quant Electron 2000;6: 462–74.
[11] Lester LF, Stintz A, Li H, Newell TC, Pease EA, Fuchs BA, et al. Optical characteristics of 1.24-μm InAs quantum-dot laser diodes. IEEE Photon Technol Lett 1999;11: 931–3.
[12] Kim JK, Naone RL, Coldren LA. Lateral carrier confinement in miniature lasers using quantum dots. IEEE J Select Top Quant Electron 2000;6:504–10.
[13] Ledentsov NN. Ordered arrays of quantum dots. In: Proc 23rd Int Conf Phys Semicond, Berlin, Germany, July, vol. 1, 1996. p. 19–26.
[14] Leonard D, Fafard S, Pond K, Zhang YH, Merz JL, Petroff PM. Structural and optical properties of self-assembled InGaAs quantum dots. J Vac Sci Technol B 1994;12(4):2516–20.
[15] Sopanen M, Taskinen M, Lipsanen H, Ahopelto J. Visible luminescence from quantum dots induced by self-organized stressors. In: Proc 23rd Int Conf Phys Semicond, Berlin, Germany, July, vol. 2, 1996. p. 1409–12.
[16] Asryan LV, Suris RA. Inhomogeneous line broadening and the threshold current density of a semiconductor quantum dot laser. Semicond Sci Technol 1996;11(4):554–67.
[17] Asryan LV, Suris RA. Temperature dependence of the threshold current density of a quantum dot laser. IEEE J Quant Electron 1998;34(5):841–50.
[18] Asryan LV, Luryi S. Tunneling-injection quantum-dot laser: ultrahigh temperature stability. IEEE J Quant Electron 2001;37(7):905–10.
[19] Agrawal GP, Dutta NK. Long-wavelength semiconductor lasers. New York: Van Nostrand Reinhold; 1986. 474 p.
[20] Welch DF, Wicks GW, Eastman LF. Calculation of the conduction band discontinuity for $Ga_{0.47}In_{0.53}As/Al_{0.48}In_{0.52}As$ heterojunction. J Appl Phys 1984;55(8): 3176–9.
[21] Adachi S. Band structure of InGaAsP [Section 17.4] In: Properties of indium phosphide. EMIS datareviews series no 6. London: INSPEC, IEE; 1991. 495 p.
[22] Nguyen LD. Properties and applications of InP-based modulation doped heterostructures [Section 7.3] In: Properties of III–V quantum wells and superlattices. EMIS datareviews series no 15. London: INSPEC, IEE; 1996. 400 p.
[23] Yoon H, Guitierrez-Aitken A, Jambunathan R, Singh J, Bhattacharya P. A "cold" InP-based tunneling injection laser with greatly reduced Auger recombination and temperature dependence. IEEE Photon Technol Lett 1992;7: 974–6.
[24] Bhattacharya P, Singh J, Yoon H, Zhang X, Gutierrez-Aitken A, Lam Y. Tunneling injection lasers: a new class of lasers with reduced hot carrier effects. IEEE J Quant Electron 1996;32:1620–9.
[25] Klotzkin D, Bhattacharya P. Temperature dependence of dynamic and DC characteristics of quantum-well and quantum-dot lasers: a comparative study. IEEE J Lightwave Technol 1999;17:1634–42.
[26] Kamath K, Klotzkin D, Bhattacharya P. Small-signal modulation characteristics of self-organized quantum dot separate confinement heterostructure and tunneling injection lasers. In: Proc of IEEE LEOS 10th Annual Meeting, San Francisco, CA, November, vol. 2, 1997. p. 498–9.
[27] Bhattacharya P, Zhang X, Yuan Y, Kamath K, Klotzkin D, Caneau C, et al. High-speed tunnel injection quantum well and quantum dot lasers. In: Proc of SPIE International Symposium PHOTONICS WEST'98, San Jose, CA, January, vol. 3283, 1998. p. 702–9.
[28] Asryan LV, Suris RA. Charge neutrality violation in quantum dot lasers. IEEE J Select Top Quant Electron 1997;3(2):148–57.
[29] Walter G, Holonyak Jr N, Ryou JH, Dupuis RD. Room-temperature continuous photopumped laser operation of coupled InP quantum dot and InGaP quantum well InP–InGaP–In(AlGa)P–InAlP heterostructures. Appl Phys Lett 2001;79(13):1956–8.
[30] Walter G, Holonyak Jr N, Ryou JH, Dupuis RD. Coupled InP quantum-dot InGaP quantum well InP–InGaP–In(AlGa)P–InAlP heterostructure diode laser operation. Appl Phys Lett 2001;79(20):3215–7.
[31] Chung T, Walter G, Holonyak Jr N. Coupled strained-layer InGaAs quantum-well improvement of an InAs quantum dot AlGaAs–GaAs–InGaAs–InAs heterostructure laser. Appl Phys Lett 2001;79(27):4500–2.
[32] Walter G, Chung T, Holonyak Jr N. High-gain coupled InGaAs quantum well InAs quantum dot AlGaAs–GaAs–InGaAs–InAs heterostructure diode laser operation. Appl Phys Lett 2002;80(7):1126–8.
[33] Chuang SL, Holonyak Jr N. Efficient quantum well to quantum dot tunneling: Analytical solutions. Appl Phys Lett 2002;80(7):1270–2.
[34] Bhattacharya P, Ghosh S. Tunnel injection $In_{0.4}Ga_{0.6}As$/GaAs quantum dot lasers with 15 GHz modulation bandwidth and $T_0 = 237$ K at room temperature, Appl Phys Lett 2002;80(19):3482–4.